

Learning quantities of interest from parametric PDEs: An efficient neural-weighted Minimal Residual approach

Ignacio Brevis⁵, Ignacio Muga¹, David Pardo^{2,3,4}, Oscar Rodríguez^{2,3}, and
Kristoffer G. van der Zee⁵

¹Instituto de Matemáticas, Pontificia Universidad Católica de Valparaíso, Chile.

²Universidad del País Vasco, Spain.

³Basque Center for Applied Mathematics, Spain.

⁴Ikerbasque, Spain.

⁵School of Mathematical Sciences, University of Nottingham, UK.

April 1, 2023

Abstract

The efficient approximation of parametric PDEs is of tremendous importance in science and engineering. In this paper, we show how one can train Galerkin discretizations to efficiently learn quantities of interest of solutions to a parametric PDE. The central component in our approach is an efficient neural-network-weighted Minimal-Residual formulation, which, after training, provides Galerkin-based approximations in standard discrete spaces that have accurate quantities of interest, regardless of the coarseness of the discrete space.

Contents

1	Introduction	2
2	Deep learning MinRes methodology	3
2.1	The abstract parametric problem	3
2.2	Main idea of Neural-weighted MinRes	4
2.3	Training of neural-weighted MinRes discrete system	5
3	Ensuring Efficiency	6
3.1	Efficient assembly: Precompute sub-domain Gram matrices	6
3.2	Efficient assembly: Precompute stiffness matrices and load vectors with unit parameters	7
3.3	Off-line procedure	8
3.4	Online procedure	8
4	Neural-Network Adaptive Training Set	9
4.1	Adaptive generation of training data	9

5	Numerical Results	10
5.1	1D diffusion-reaction equation with one parameter	11
5.2	1D diffusion-reaction equation with two parameters	12
5.3	1D advection with parametric right-hand side	14
5.4	2D discontinuous-media diffusion equation with two parameters	16
6	Conclusions	18

1 Introduction

How to learn a reduced order model for parametric partial differential equations (PDEs) given pairs of parameters and solution observations? This question has received significant attention in recent years, where a common theme is the hybrid use of neural networks and classical approximations. The aim of this work is to present a new hybrid methodology, based on a neural-network-weighted Minimal Residual (MinRes) Galerkin discretization, that efficiently learns quantities of interest of the PDE solution.

A currently well-established hybrid paradigm for parametric PDEs is to train a neural network to find the coefficients that define an element in a discrete solution space. Effectively, the neural network provides an approximation to the parameter-to-solution map, i.e., the operator that maps parameters to solutions. This has been well explored in the context of non-intrusive Reduced-Basis methods [8,12,16], where the discrete space is the span of solution snapshots (reduced basis space); see also [1,4,22] for related approaches and discussions. More recent is the idea to simply apply this paradigm to the full discrete finite element space [9,13,27], cf. [17]. A disadvantage in these approaches is that the approximations that are produced are no longer guaranteed to satisfy the Galerkin equations of the underlying weak formulation.¹

Because these approaches provide a complete operator-approximation, significant amounts of data may be required to learn it (i.e., to train the neural network). Much less data is expected to be needed to approximate the parameter-to-*quantity-of-interest* map, which is the operator that maps PDE parameters to output quantities of interest (in \mathbb{R}) of the PDE solution. This has been explored by, e.g., Khoo, Lu & Ying [14], who use a neural network to map the PDE parameters directly into such quantities. In that approach, there is however no PDE solution approximation.

The objective of this paper is to presents for parametric PDEs, a deep learning methodology for obtaining Galerkin-based approximations in standard discrete spaces that have accurate quantities of interest, regardless of the coarseness of the discrete space. More precisely, the methodology provides an approximation to the parameter-to-quantity-of-interest map, by delivering Galerkin-based approximations on a fixed discrete space for a neural-network-weighted weak formulation. During the (supervised) training, a discrete method is learned by optimizing a weight-function within the formulation. This guarantees that its Galerkin approximations are tailored towards the desired quantities of interest.

We employ a weighted Minimal Residual weak formulation, where the weight function is defined by a neural network. This ensures that for arbitrary weight functions, the resulting Galerkin formulation remains stable and consistent. The theory of Minimal Residual formulations has its origin in the discontinuous Petrov–Galerkin method developed by Demkowicz, Gopalakrisnan et al [5,6].

¹In fact, for non-intrusive reduced basis methods, the key motivation is to avoid setting up the Galerkin equations (in the reduced basis space) in order to be non-intrusive.

Our methodology can be viewed as one where a numerical method is optimized amongst a family of methods, and which utilizes a neural network to learn the optimal method. These ideas go back to Mishra [18], who proposed such learning for families of finite differences methods for PDEs. Similar work on optimizing numerical methods can be found in, e.g. [24, 26]. Our current work is a continuation of our previous works [2] and [3], where we presented a weighted MinRes formulation for the case of parameter dependence in the right-hand-side only, and where we analyzed the well-posedness and convergence in the non-parametric case, respectively.

The main contributions in our current work are as follows. Firstly, we propose the neural-weighted MinRes approach for an abstract and general parametric PDE. Secondly, we propose new weight functions that depend on the neural network, which lead to piecewise-weighted inner products and allow the practical assembly needed in the training stage.² We demonstrate fully-efficient off-line and on-line procedures in the case of affine parameter dependence. Thirdly, we propose an adaptive generation of the training set to allow for greedy selection of data. This ensure efficient convergence of errors in the quantity of interest.

The contents of the paper are as follows: Section 2 presents the deep learning methodology for the neural-weighted MinRes formulation. Section 3 presents details that demonstrate the efficiency of all involved matrix assemblies, the off-line procedure and on-line procedure. Section 4 presents the adaptive training set approach. Section 5 contains numerical experiments. Finally, Section 6 discusses conclusions.

2 Deep learning MinRes methodology

2.1 The abstract parametric problem

Let \mathbb{U} and \mathbb{V} be infinite-dimensional Hilbert spaces, with their respective dual spaces \mathbb{U}^* and \mathbb{V}^* . Given a bounded set of parameters $\Lambda \subset \mathbb{R}^\rho$, we consider parametric families of bounded invertible linear operators $B_\lambda : \mathbb{U} \rightarrow \mathbb{V}^*$, and continuous linear functionals $\ell_\lambda : \mathbb{V} \rightarrow \mathbb{R}$, where $\lambda \in \Lambda$. Consequently, we define the parametric family of problems:

$$\begin{cases} \text{Given } \lambda \in \Lambda, \text{ find } u_\lambda \in \mathbb{U} \text{ such that} \\ B_\lambda u_\lambda = \ell_\lambda \text{ in } \mathbb{V}^*. \end{cases} \quad (1)$$

Problems like (1) are commonly found in variational formulations of parametric PDEs, in which case the linear operator B_λ is defined through a parametrized bilinear form $b_\lambda : \mathbb{U} \times \mathbb{V} \rightarrow \mathbb{R}$ such that $\langle B_\lambda u, v \rangle_{\mathbb{V}^*, \mathbb{V}} := b_\lambda(u, v)$.

In many applications, the interest is not focused on the whole solution u_λ of problem (1), but in a quantity of interest $q(u_\lambda)$, where $q : \mathbb{U} \rightarrow \mathbb{R}$ is a given functional of interest³ (linear or non-linear). In such situations, we are more interested in reproducing the mapping

$$\Lambda \ni \lambda \mapsto q_\lambda := q(u_\lambda) \in \mathbb{R}, \quad \text{where } u_\lambda \text{ solves (1).}$$

²And suitable for automatic differentiation in, e.g., Tensorflow.

³For instance, the evaluation of the solution at a single point, or the average of the solution in some portion of its domain.

2.2 Main idea of Neural-weighted MinRes

To approximate $u_\lambda \in \mathbb{U}$ solution of (1), we use the following mixed (saddle-point) formulation:

$$\left\{ \begin{array}{l} \text{Find } (r_\lambda^m, u_\lambda^n) \in \mathbb{V}^m \times \mathbb{U}^n \text{ s.t.} \\ (r_\lambda^m, v^m)_{\omega_\lambda} + \langle B_\lambda u_\lambda^n, v^m \rangle_{\mathbb{V}^*, \mathbb{V}} = \langle \ell_\lambda, v^m \rangle_{\mathbb{V}^*, \mathbb{V}}, \quad \forall v^m \in \mathbb{V}^m, \\ \langle B_\lambda w^n, r_\lambda^m \rangle_{\mathbb{V}^*, \mathbb{V}} = 0, \quad \forall w^n \in \mathbb{U}^n. \end{array} \right. \quad (2)$$

In the above expression,

- \mathbb{V}^m and \mathbb{U}^n denote conforming discretizations of \mathbb{V} and \mathbb{U} , such that $m = \dim \mathbb{V}^m > \dim \mathbb{U}^n = n$;
- $(\cdot, \cdot)_{\omega_\lambda}$ denotes an equivalent⁴ weighted inner product on \mathbb{V} , with a λ -dependent weight ω_λ ;
- $\langle \cdot, \cdot \rangle_{\mathbb{V}^*, \mathbb{V}}$ denotes the standard duality pairing between \mathbb{V}^* and \mathbb{V} .
- $u_\lambda^n \in \mathbb{U}^n$ is the approximation to the exact solution $u_\lambda \in \mathbb{U}$; and
- $r_\lambda^m \in \mathbb{V}^m$ is the representative of the residual $\ell_\lambda - B_\lambda u_\lambda^n \in (\mathbb{V}^m)^*$ under the weighted inner-product $(\cdot, \cdot)_{\omega_\lambda}$.

The main idea of neural-weighted MinRes is to work with a trainable weight function ω_λ , that can be trained to minimize errors of u_λ^n in the quantity of interest, i.e.,

$$\frac{1}{2} |q(u_\lambda^n) - q_\lambda|^2 \rightarrow \min. \quad (3)$$

The details about the training process can be found in Section 2.3.

The acronym MinRes in this methodology comes from the fact that the mixed formulation (2) corresponds to the saddle point formulation of the residual minimization problem

$$u_\lambda^n := \operatorname{argmin}_{w^n \in \mathbb{U}^n} \|\ell_\lambda - B_\lambda w^n\|_{(\mathbb{V}^m)^*} = \operatorname{argmin}_{w^n \in \mathbb{U}^n} \sup_{v^m \in \mathbb{V}^m} \frac{\langle \ell_\lambda - B_\lambda w^n, v^m \rangle_{\mathbb{V}^*, \mathbb{V}}}{\sqrt{(v^m, v^m)_{\omega_\lambda}}}. \quad (4)$$

Notice that the norm on $(\mathbb{V}^m)^*$ is computed through the norm on \mathbb{V} induced by the weighted inner-product $(\cdot, \cdot)_{\omega_\lambda}$.

We refer the reader to [19] for a concise and detailed explanation of the equivalences between (2) and (4), and also with the Petrov–Galerkin method with optimal test functions.

Example 2.1. *In an H_0^1 context (i.e., $\mathbb{V} = H_0^1(\Omega)$ for $\Omega \subset \mathbb{R}^d$), we can use a positive weight function $\omega_\lambda \in L^\infty(\Omega)$ and define the weighted H_0^1 inner-product*

$$(f, g)_{\omega_\lambda} := \int_{\Omega} \omega_\lambda(x) \nabla f(x) \cdot \nabla g(x) dx. \quad (5)$$

Of course, the weight ω_λ depends on the set of parameters $\lambda \in \Lambda$ and must also depend on a set of trainable parameters $\theta \in \Theta$. That is, $\omega_\lambda = \omega_\lambda(x; \theta)$.

⁴Equivalent in the sense that it produces the same topology as the original inner product of \mathbb{V} does.

2.3 Training of neural-weighted MinRes discrete system

We choose artificial neural networks [10] to train the weight function ω_λ due to their well-known expressivity properties [11,23]. Since $(r_\lambda^m, u_\lambda^n)$ in (2) depends on the inner-product weight ω_λ , then it will also depend on any trainable parameter $\theta \in \Theta$ of such weight. Thus, in some cases we write $u_\lambda^n := u_\lambda^n(\theta)$ and $r_\lambda^m := r_\lambda^m(\theta)$ to make this dependency explicit. More details on how we choose the weight function to ensure efficiency can be found in the next Section 3.

Consider now sets of basis function such that $\mathbb{U} = \text{span}\{\varphi_1, \dots, \varphi_n\}$ and $\mathbb{V}^m = \text{span}\{\psi_1, \dots, \psi_m\}$. Thus, system (2) can be rewritten as:

$$\left\{ \begin{array}{l} \text{Find } (\vec{r}(\lambda), \vec{u}(\lambda)) \in \mathbb{R}^m \times \mathbb{R}^n \text{ s.t.} \\ \left[\begin{array}{c|c} \mathbb{G}_\lambda(\theta) & \mathbb{B}_\lambda \\ \hline \mathbb{B}_\lambda^\top & 0 \end{array} \right] \begin{bmatrix} \vec{r}(\lambda) \\ \vec{u}(\lambda) \end{bmatrix} = \begin{bmatrix} \vec{L}_\lambda \\ 0 \end{bmatrix}, \end{array} \right. \quad (6)$$

where

$$r_\lambda^m = \sum_{i=1}^m r_i(\lambda) \psi_i \quad \text{and} \quad u_\lambda^n = \sum_{j=1}^n u_j(\lambda) \varphi_j.$$

Notice that

- \mathbb{G}_λ is the Gram matrix obtained from the evaluation of the weighted inner product in the test-space basis functions, i.e., $(\mathbb{G}_\lambda)_{ik} = (\psi_k, \psi_i)_{\omega_\lambda}$;
- \mathbb{B}_λ denotes the $m \times n$ matrix obtained from the evaluation of the operator $B_\lambda : \mathbb{U} \rightarrow \mathbb{V}^*$ in the basis functions, i.e., $(\mathbb{B}_\lambda)_{ij} = \langle B_\lambda \varphi_j, \psi_i \rangle_{\mathbb{V}^*, \mathbb{V}}$; and
- \vec{L}_λ represents the load vector computed from the evaluation of the test-space basis functions into the right-hand functional $\ell_\lambda \in \mathbb{V}^*$, i.e., $(\vec{L}_\lambda)_i = \ell_\lambda(\psi_i)$.

Notice that our approximate quantity of interest $q(u_\lambda^n)$ can be computed in the following way:

$$q(u_\lambda^n) = q\left(\sum_{j=1}^n u_j(\lambda) \varphi_j\right) = \sum_{j=1}^n u_j(\lambda) q(\varphi_j) = \vec{u}(\lambda) \cdot \vec{q},$$

where $\vec{q} = (q(\varphi_1), \dots, q(\varphi_n))$.

To find an optimal inner-product weight ω_λ^* , minimizing (3), we need to train the artificial neural network associated with the trainable parameters $\theta \in \Theta$ of the weight. The training procedure is executed by minimizing the following cost functional:

$$\mathcal{L}(\theta; \{\lambda_i, q_{\lambda_i}\}_{i=1}^{N_s}) := \frac{1}{N_s} \sum_{i=1}^{N_s} \frac{1}{2} \left| \frac{q_{\lambda_i} - \vec{u}(\lambda_i; \theta) \cdot \vec{q}}{q_{\lambda_i}} \right|^2, \quad (7)$$

where $\{\lambda_i\}_{i=1}^{N_s} \subset \Lambda$ is a set of parameters and $\{q_{\lambda_i}\}_{i=1}^{N_s}$ is an associated set of reliable quantities of interest (also referred to as *labels*, see, e.g. [10,20]). The training set $\{\lambda_i, q_{\lambda_i}\}_{i=1}^{N_s}$ can be generated in several ways depending on the nature of the physical problem. For example, from measurements or observations, or it can be computed using high-precision numerical schemes.

Figure 1 summarizes the training procedure, describing the process at each epoch. That is, given $\theta \in \Theta$, we build the weight function $\omega_\lambda(\theta)$. For each λ_i in the training set, we solve the system (6) to compute $u_{\lambda_i}^n$ using the weighted inner product associated with the weight $\omega_{\lambda_i}(\theta)$. Finally, the cost functional (7) is used to update the value of θ , and repeat.

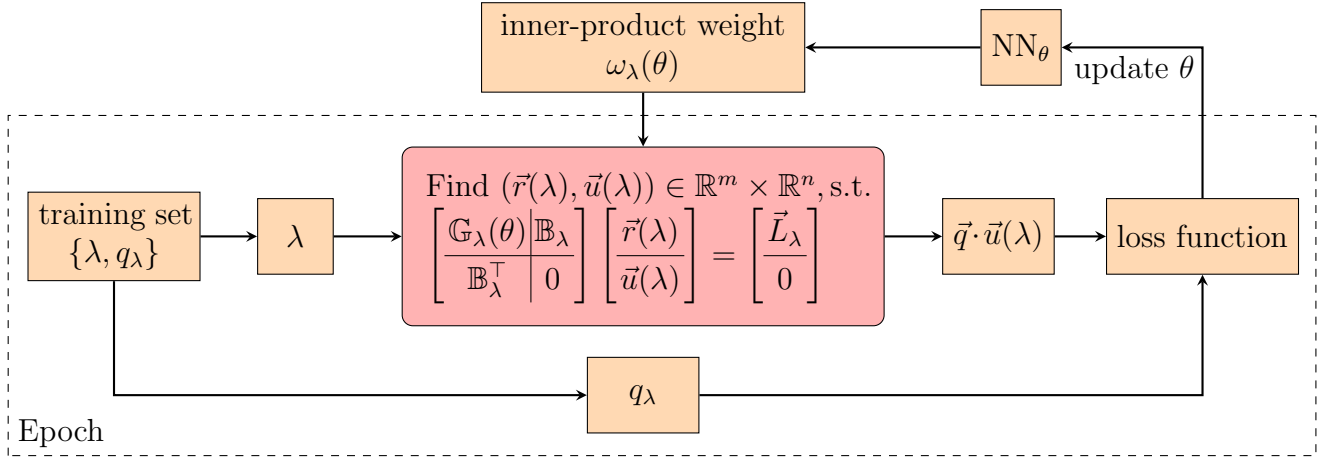


Figure 1: Supervised training process for the artificial neural network and the inner-product weight.

3 Ensuring Efficiency

3.1 Efficient assembly: Precompute sub-domain Gram matrices

We will work with variational formulations of PDEs. Hence, as in Example 2.1, our inner products must depend on the PDE domain variable, say $x \in \Omega \subset \mathbb{R}^d$. Moreover, we want to use conforming piecewise polynomial approximation spaces for \mathbb{U}^n and \mathbb{V}^m . In particular, to assemble the Gram matrix \mathbb{G}_λ in (6), we need to compute the inner products $(\mathbb{G}_\lambda)_{ik} = (\psi_k, \psi_i)_{\omega_\lambda}$ for every value of λ in the training set, for every trainable parameter θ under consideration, and for every pair of piecewise polynomial test-space basis functions in $\{\psi_1, \dots, \psi_m\}$. This could be an extremely expensive task for L^2 -based inner products like (5). To overcome these difficulties, we propose the following strategies:

- Let Ω_h be a partition of Ω , defined as a collection of finite many open connected elements $T \subset \Omega$ with Lipschitz boundaries, such that $\overline{\Omega} = \cup_{T \in \Omega_h} \overline{T}$.
- Define a discrete test space $\mathbb{V}^m \subset \mathbb{V}$ as a conforming piecewise polynomial space over the mesh Ω_h .
- Define a (coarser) discrete trial space \mathbb{U}^n as a conforming piecewise polynomial space over the mesh Ω_h .
- Define a non-overlapping domain decomposition of Ω , consisting of n_a patches $\{\Omega_l\}_{l=1}^{n_a}$ of elements of Ω_h , such that $\cup_{l=1}^{n_a} \overline{\Omega}_l = \overline{\Omega}$.
- In terms of the PDE variable $x \in \Omega$, the weight function $\omega_\lambda(x; \theta)$ will be a positive piecewise polynomial function defined on the patches $\{\Omega_l\}_{l=1}^{n_a}$, i.e., $\omega_\lambda(\cdot; \theta)|_{\Omega_l}$ is a polynomial of degree $p \in \mathbb{N}$.
- In terms of the PDE parameter $\lambda \in \Lambda$, the weight function $\omega_\lambda(x; \theta)$ will be a neural network, whose input parameters are λ and the patch index $l \in \{1, \dots, n_a\}$, and whose output parameters are the coefficients of the polynomial $\omega_\lambda(\cdot; \theta)|_{\Omega_l}$ in some basis expansion (θ is the trainable parameter).

With this setting, the computation of coefficients $(\mathbb{G}_\lambda)_{ik}$ of the Gram matrix becomes a piecewise polynomial integration, where we can use quadrature rules to perform exact computations (avoiding the uncertain problem of integrating a neural network; see, e.g., [25]). However, the main advantage is that we can pre-assemble the Gram matrix before training in order to avoid integration routines during the training procedure. To fix ideas, let $\{\phi_{l1}, \dots, \phi_{ln_p}\}$ be a basis of the space of polynomial of order p over Ω_l . Thus, we write

$$\omega_\lambda(x; \theta)|_{\Omega_l} = \sum_{j=1}^{n_p} c_j(\lambda, l; \theta) \phi_{lj}(x), \quad (8)$$

where $\{c_j(\lambda, l; \theta)\}_{j=1}^{n_p}$ are the outputs of the neural network.

Remark 3.1. *As an alternative, we can use neural networks whose input parameter is λ , and whose output is the whole set of $n_a \times n_p$ polynomial coefficients $\cup_{l=1}^{n_a} \{c_j(\lambda, l; \theta)\}_{j=1}^{n_p}$.*

Consider the following explanatory example.

Example 3.1. *In the same context of Example 2.1, let $\mathbb{V}^m := \text{span}\{\psi_1, \dots, \psi_m\} \subset H_0^1(\Omega)$. In this case, using the expression (8), the coefficients of the Gram matrix become*

$$\begin{aligned} (\mathbb{G}_\lambda)_{ik} &= (\psi_k, \psi_i)_{\omega_\lambda} = \sum_{l=1}^{n_a} \int_{\Omega_l} \omega_\lambda(x; \theta) \nabla \psi_k(x) \cdot \nabla \psi_i(x) dx \\ &= \sum_{l=1}^{n_a} \sum_{j=1}^{n_p} c_j(\lambda, l; \theta) \underbrace{\int_{\Omega_l} \phi_{lj}(x) \nabla \psi_k(x) \cdot \nabla \psi_i(x) dx}_{=:(\mathbb{M}^{lj})_{ik}}, \end{aligned}$$

where $(\mathbb{M}^{lj})_{ik}$ corresponds to one coefficient of a (sparse) sub-domain Gram matrix \mathbb{M}^{lj} , which can be pre-assembled before training using exact quadrature rules. Therefore, at each Epoch and for any λ , the full Gram matrix can be rapidly assembled using the formula

$$\mathbb{G}_\lambda(\theta) = \sum_{l=1}^{n_a} \sum_{j=1}^{n_p} c_j(\lambda, l; \theta) \mathbb{M}^{lj}.$$

Remark 3.2 (Practical piecewise polynomial weights). *In practice, to ensure positive polynomials in (8), we use polynomial order up to $p = 1$. The reason is that positive constants $c_j(\lambda, l; \theta)$ describe all positive linear polynomials when using nodal basis functions on simplices. A similar situation occurs for piecewise constants, i.e., when $p = 0$. However, describing the set of all positive polynomials in higher degrees is on another level of complexity.*

3.2 Efficient assembly: Precompute stiffness matrices and load vectors with unit parameters

Recall from Section 2.3 that we are also working with a $m \times n$ matrix \mathbb{B}_λ resulting from the evaluation of the operator $B_\lambda : \mathbb{U} \rightarrow \mathbb{V}^*$ in the basis functions of the discrete spaces \mathbb{U}^n and \mathbb{V}^m . That is, $(\mathbb{B}_\lambda)_{ij} := \langle B_\lambda \varphi_j, \psi_i \rangle_{\mathbb{V}^*, \mathbb{V}}$ where $\text{span}\{\varphi_1, \dots, \varphi_n\} = \mathbb{U}^n$ and $\text{span}\{\psi_1, \dots, \psi_m\} = \mathbb{V}^m$.

We further assume that the operator B_λ allows an affine decomposition of the form

$$B_\lambda = B_0 + \sum_{l=1}^{n_b} \Phi_l(\lambda) B_l,$$

where $\{B_l : \mathbb{U} \rightarrow \mathbb{V}^*\}_{l=0}^{n_b}$ are continuous linear operators (independent from λ) and $\{\Phi_l : \Lambda \rightarrow \mathbb{R}\}_{l=1}^{n_b}$ are given functions of the set of parameters. Naturally, this will induce a self-explained matrix decomposition of the form

$$\mathbb{B}_\lambda = \mathbb{B}_0 + \sum_{l=1}^{n_b} \Phi_l(\lambda) \mathbb{B}_l, \quad (9)$$

where the matrices $\{\mathbb{B}_l\}_{l=0}^{n_b}$ can be pre-assembled before training following the same idea of the previous Section 3.1.

The same assumption is made on the parametrized right-hand side functional $\ell_\lambda \in \mathbb{V}^*$. Namely, express $\ell_\lambda = \ell_0 + \sum_{l=1}^{n_l} \Psi_l(\lambda) \ell_l$; next define loading vectors

$$\vec{L}_\lambda = \vec{L}_0 + \sum_{l=1}^{n_l} \Psi_l(\lambda) \vec{L}_l; \quad (10)$$

and proceed as before pre-assembling λ -independent vectors before training.

3.3 Off-line procedure

Once we have performed all the pre-assemblies described in previous Sections 3.1 and 3.2, we start defining the neural network and its training settings, i.e., the neural network architecture (which contains the trainable parameters) and the training algorithm with its hyperparameters (non-trainable parameters). We observe two main possible architectures (cf. Eq.(8) and Remark 3.1):

- $\lambda \rightarrow \text{NN}(\lambda; \theta) \rightarrow \bigcup_{l=1}^{n_a} \{c_j(\lambda, l; \theta)\}_{j=1}^{n_p}$; and
- $(\lambda, l) \rightarrow \text{NN}(\lambda, l; \theta) \rightarrow \{c_j(\lambda, l; \theta)\}_{j=1}^{n_p}$.

Defining a training set $\{\lambda_i, q_{\lambda_i}\}_{i=1}^{N_s}$ (and a validation set if necessary), we train the neural network by minimizing the loss function (7). This loss will deliver the trained parameter of the neural network, i.e.,

$$\theta^* = \underset{\theta \in \Theta}{\operatorname{argmin}} \mathcal{L}(\theta, \{\lambda_i, q_{\lambda_i}\}_{i=1}^{N_s}) := \underset{\theta \in \Theta}{\operatorname{argmin}} \frac{1}{N_s} \sum_{i=1}^{N_s} \frac{1}{2} \left| \frac{q_{\lambda_i} - \vec{u}(\lambda_i; \theta) \cdot \vec{q}}{q_{\lambda_i}} \right|^2. \quad (11)$$

We emphasize that the cost functional \mathcal{L} is constrained by the linear system (6). Additionally, in Section 4 we describe an adaptive training procedure that can be used to improve the performance of the trained neural network.

3.4 Online procedure

With the trained parameter θ^* in hand (see equation (11)), for any $\lambda \in \Lambda$ we solve the system

$$\left[\begin{array}{c|c} \mathbb{G}_\lambda(\theta^*) & \mathbb{B}_\lambda \\ \hline \mathbb{B}_\lambda^\top & 0 \end{array} \right] \left[\begin{array}{c} \vec{r}(\lambda) \\ \vec{u}(\lambda) \end{array} \right] = \left[\begin{array}{c} \vec{L}_\lambda \\ 0 \end{array} \right], \quad (12)$$

and finally compute $\vec{q} \cdot \vec{u}(\lambda)$ as an approximation of the exact quantity of interest $q_\lambda = q(u_\lambda)$.

4 Neural-Network Adaptive Training Set

In classical training for machine learning models, we usually rely on a fixed amount of observations, which are splitted between training and validation sets (sometimes also on a test set). However, with the increasing machine learning models, different approaches to training were developed. Those techniques range from avoiding overfitting from large amount of data, to avoiding underfitting by generating new data from small training sets. The training time and final result of the training process will depend, among other elements, on the election of an adequate training set. Some well-known methodologies of adaptive training set are bootstrapping in neural networks [7], important sampling [21], and mesh refinement in PINNs [28]. We implement a methodology to add samples to training and validation sets at specific training epochs.

4.1 Adaptive generation of training data

We employ an adaptive training step to improve the training process without significantly increasing computational cost. Based on the idea of adaptive integration presented in [25], we define an adaptive training set that will iteratively incorporate the elements of the validation set with the worst performance (accordingly to certain criteria). Particularly in this work, we include in the training set those elements of the validation with a loss evaluation greater than γ times the loss of the training set. Algorithm 1 describes this idea.

Algorithm 1 Adaptivity for the training set

Require: $X_{\text{train}}, X_{\text{val}}, \gamma$

```
while stage < #stages do                                ▷ #stages: number of stages to update the training set
  while epoch < #epochs do                                ▷ #epochs: number of epochs
     $\theta^* \leftarrow \operatorname{argmin}_{\theta} \mathcal{L}(\theta; X_{\text{train}})$     ▷ neural network training
  end while
   $\mathcal{L}_{\text{train}} \leftarrow \mathcal{L}(\theta^*; X_{\text{train}})$ 
  for  $x_{\text{val}} \in X_{\text{val}}$  do
    if  $\mathcal{L}(\theta^*; \{x_{\text{val}}\}) > \gamma \mathcal{L}_{\text{train}}$  then    ▷ Chosen criteria
       $X_{\text{train}} \leftarrow X_{\text{train}} \cup \{x_{\text{val}}\}$ 
    end if
  end for
  update  $X_{\text{val}}$                                           ▷  $X_{\text{val}}$  is updated when new points are added to  $X_{\text{train}}$ 
end while
```

Remark 4.1. *If γ is greater than one, we avoid overfitting by adding the validation-set points with a loss value that lags behind the training-set loss value.*

We propose as validation set the middle points (center of mass in higher dimensions) of the elements in the training. So each time that a validation-set point is included as part the training set, we update the validation set adding the new middle point from the training set. Figure 2 illustrate the procedure of training and validation set updates. For example,

1. Select a training set from coarse grid of the parameter space Λ .
2. We define the validation set as the middle points of the coarse grid.

3. Run a usual minimization method (SDG, Adam, RMSProp, etc) to train the artificial neural network with the above training set for a certain number of epochs.
4. Evaluate the loss function within the elements of the validation set.
5. Add the validation-set points with worst results to the training set (according to certain criteria, see Algorithm 1).
6. Update the validation set by removing the points added to the training set and adding the new needed middle points.

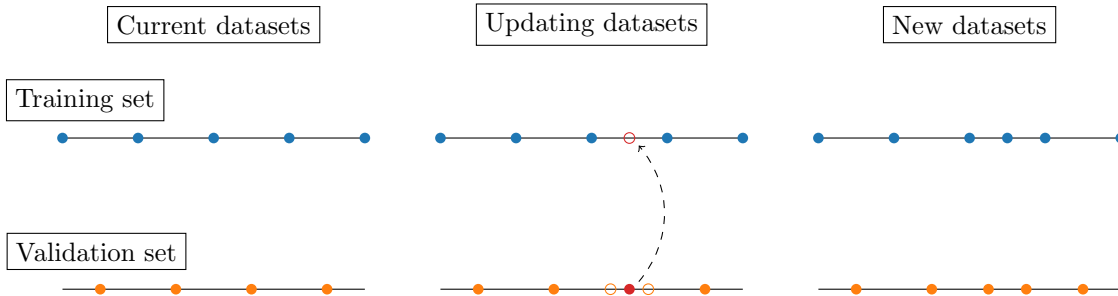


Figure 2: Adaptive training and validation sets.

5 Numerical Results

We present some numerical examples to show the different features of the method. In the next examples, unless otherwise stated, we employ feed-forward neural networks with three hidden layers and ten neurons on each hidden layer. The input of the neural network is the PDE parameter λ , then the input layer of the neural network has ρ neurons (with $\rho := \dim \Lambda$). The output of the neural network is the set of coefficients associated with the weighted inner product. Thus, for a piecewise constant weight function (i.e., $p = 0$) defined on n_a patches, the output layer contains n_a neurons, i.e.,

$$\lambda \longrightarrow \text{NN}(\lambda; \theta) \longrightarrow \{c(\lambda, 1; \theta), \dots, c(\lambda, n_a; \theta)\}.$$

To ensure positive constants, we choose the softplus function as the activation function for the output layer (while the hyperbolic tangent function is used on every other layer). To train the neural network, we employ the Adam optimization algorithm [15] within TensorFlow, with decay rates $\beta_1 = 0.9$ and $\beta_2 = 0.999$, regularization term for numerical stability $\epsilon = 1e^{-16}$, EMA momentum equal to 0.99, and learning rate $\alpha = 1.e^{-4}$. Table 1 displays a TensorFlow scheme of the neural network architecture.

ML-MinRes neural network architecture		
Layer (type)	Output Shape	Activation Function
Input non-trainable layer (λ)	(None, ρ)	tanh
Hidden Dense layer	(None, 10)	tanh
Hidden Dense layer	(None, 10)	tanh
Hidden Dense layer	(None, 10)	tanh
Output Dense layer (c)	(None, n_a)	softplus

Table 1: Neural network architecture employed in most of the following examples.

5.1 1D diffusion-reaction equation with one parameter

We consider a 1D diffusion-reaction equation with the parameter λ in the reaction term. The right-hand side of this problem is given by a Dirac delta function located at $x_0 = 0.6$. Thus, we have the following problem:

$$\begin{cases} -u_{xx}(x) + \lambda^2 u(x) = \delta_{x_0}(x) & \text{in } (0, 1), \\ u(0) = 0, \\ u'(1) = 0, \end{cases} \quad (13)$$

with $\lambda \in [1, 10]$. We also define the linear quantity of interest $q : \mathbb{U} \rightarrow \mathbb{R}$ as

$$q(u) = u(0.7).$$

Notice that the exact solution to problem (13) is:

$$u_\lambda(x) = \begin{cases} c_1(\exp(\lambda x) - \exp(-\lambda x)), & \text{if } x < x_0, \\ c_2(\exp(\lambda x) + \exp(\lambda(2-x))), & \text{if } x > x_0, \end{cases}$$

where

$$c_1 = \frac{1}{2\lambda} \frac{\exp(\lambda x_0) + \exp(\lambda(2-x_0))}{1 + \exp(2\lambda)} \quad \text{and} \quad c_2 = \frac{1}{2\lambda} \frac{\exp(\lambda x_0) - \exp(-\lambda x_0)}{1 + \exp(2\lambda)}.$$

Given the continuous trial and test spaces $\mathbb{U} = \mathbb{V} = H_{(0)}^1(0, 1)$, we introduce the following variational formulation of problem (13):

$$\begin{cases} \text{Find } u \in \mathbb{U} \text{ such that:} \\ \underbrace{\int_0^1 u_x v_x}_{\langle B_0 u, v \rangle_{\mathbb{V}^*, \mathbb{V}}} + \lambda^2 \underbrace{\int_0^1 uv}_{\langle B_1 u, v \rangle_{\mathbb{V}^*, \mathbb{V}}} = v(x_0), \quad \forall v \in \mathbb{V}. \end{cases} \quad (14)$$

Thus, we define $B_\lambda : \mathbb{U} \rightarrow \mathbb{V}^*$ as $B_\lambda := B_0 + \lambda^2 B_1$ and $\ell_\lambda := \delta_{x_0}$ (which is independent from λ).

In addition, we define the weighted inner product for the test space as

$$(r, v)_{\omega_{\text{pw}}} := \int_0^1 \omega_{\text{pw}}(x, \lambda) (r_x(x) v_x(x) + r(x) v(x)) dx, \quad \forall r, v \in \mathbb{V}, \quad (15)$$

with the following piecewise constant inner-product weight:

$$\omega_{\text{pw}}(x, \lambda) := \begin{cases} c(\lambda, 1), & \text{if } x \in (0, 1/4), \\ c(\lambda, 2), & \text{if } x \in (1/4, 1/2), \\ c(\lambda, 3), & \text{if } x \in (1/2, 3/4), \\ c(\lambda, 4), & \text{if } x \in (3/4, 1). \end{cases} \quad (16)$$

The discrete trial space \mathbb{U}^n will be the space generated by the function $\varphi(x) = x$, while the discrete test space \mathbb{V}^m will consist of conforming piecewise linear functions over a uniform mesh of four elements. With all these ingredients we construct the mixed formulation (2) and proceed with the methodology described in Section 2. We use the neural network architecture described in Table 1 and no adaptive training has been performed for this case. The training set is composed of $N_s = 10$ elements, such that $\lambda \in \{1, 2, 3, \dots, 10\}$.

Figure 3 shows the performance of ML-MinRes or weighted-Minres (w-MinRes) method, after training the inner-product weight for the example described above. Subfigures 3a, 3b, and 3c show the results for the classical MinRes and the ML-MinRes methods for $\lambda \in \{1.5, 5.5, 9.5\}$. In blue, we observe the discrete solution computed from solving the system (2) with the optimal inner-product weight. In orange, we show the standard minimal residual scheme (with only one element). In black dashed line, we plot the exact solution to problem (13) as a reference. The grey dashed line shows the quantity of interest location. Subfigure 3d shows the relative error in linear scale for a fine-grid test set (grid for Λ) and also display the training points. Subfigure 3e compares the relative error in logarithmic scale between the MinRes and ML-MinRes methods for a fine-grid test set. The last subfigure shows the loss function through epochs. Notice that for this training we employed three different learning rates [$1e^{-3}$, $1e^{-4}$, $1e^{-5}$], each one for 10.000 iterations, in order to avoid oscillations in the loss function.

5.2 1D diffusion-reaction equation with two parameters

We consider 1D diffusion-reaction problem with a two-dimensional parameter $\lambda = (\alpha, \beta)$. The right-hand side of this problem is given by a Dirac delta function located at $x_0 = 0.6$. The first component of the parameter α multiplies the diffusion term and the second component β multiplies the reaction term. Thus, we have the following problem:

$$\begin{cases} -\alpha^2 u_{xx}(x) + \beta^2 u(x) = \delta_{x_0}(x), & \text{in } (0, 1). \\ u(0) = 0, \\ u'(1) = 0, \end{cases} \quad (17)$$

with $\lambda = (\alpha, \beta) \in [1, 10]^2$. We set the quantity of interest as $q(u) = u(0.7)$. Notice that the exact solution to this problem (17) is

$$u_\lambda(x) = \begin{cases} c_1 \left(\exp\left(\frac{\beta}{\alpha}x\right) - \exp\left(-\frac{\beta}{\alpha}x\right) \right), & \text{if } x < x_0, \\ c_2 \left(\exp\left(\frac{\beta}{\alpha}x\right) + \exp\left(\frac{\beta}{\alpha}(2-x)\right) \right), & \text{if } x > x_0, \end{cases} \quad (18)$$

where

$$c_1 = \frac{1}{2\alpha\beta} \frac{\exp\left(\frac{\beta}{\alpha}x_0\right) + \exp\left(\frac{\beta}{\alpha}(2-x_0)\right)}{1 + \exp\left(2\frac{\beta}{\alpha}\right)} \quad \text{and} \quad c_2 = \frac{1}{2\alpha\beta} \frac{\exp\left(\frac{\beta}{\alpha}x_0\right) - \exp\left(-\frac{\beta}{\alpha}x_0\right)}{1 + \exp\left(2\frac{\beta}{\alpha}\right)}.$$

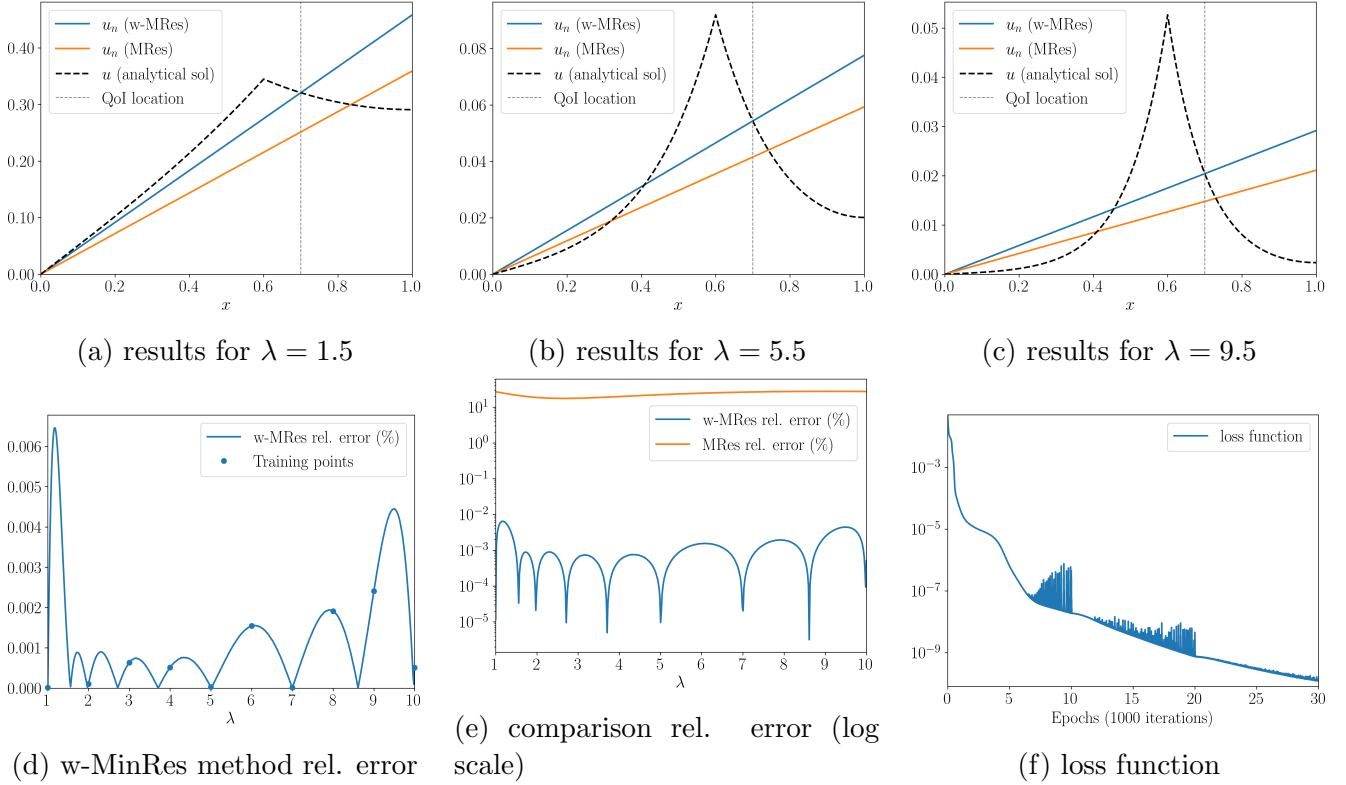


Figure 3: ML-MinRes performance for 1D parametric diffusion reaction example.

As in the previous example, we set the trial and test spaces to be $\mathbb{U} = \mathbb{V} = H^1_{(0)}(0, 1)$, and the variational formulation is given by

$$\left\{ \begin{array}{l} \text{Find } u \in \mathbb{U} \text{ such that:} \\ \alpha^2 \underbrace{\int_0^1 u_x v_x}_{\langle B_1 u, v \rangle_{\mathbb{V}^*, \mathbb{V}}} + \beta^2 \underbrace{\int_0^1 uv}_{\langle B_2 u, v \rangle_{\mathbb{V}^*, \mathbb{V}}} = v(x_0), \quad \forall v \in \mathbb{V}. \end{array} \right. \quad (19)$$

Thus, we define $B_\lambda : \mathbb{U} \rightarrow \mathbb{V}^*$ as $B_\lambda := \alpha^2 B_1 + \beta^2 B_2$ and $\ell_\lambda := \delta_{x_0}$ (which is independent from λ). In addition, we use the same inner product defined in (15)-(16), together with the same (discrete) trial and test space of the previous example in Section 5.1.

Notice that in this example, the artificial neural network has two neurons in the input layer (and four in the output layer). For the training set, we select 100 equispaced elements in the set $(1, 10) \times (1, 10)$ (see red dots in Subfigure 4b). In addition, we employed three different learning rates $[1e^{-3}, 1e^{-4}, 1e^{-5}]$ during the training, each one for 15.000 iterations.

Subfigure 4a displays the loss function through epochs for the three different learning rates $[1e^{-3}, 1e^{-4}, 1e^{-5}]$. Subfigure 4b shows the relative error in linear scale for a test set (fine-grid in Λ) and also display the training points in red dots. The picture shows that the relative error is below 0.5% after the training.

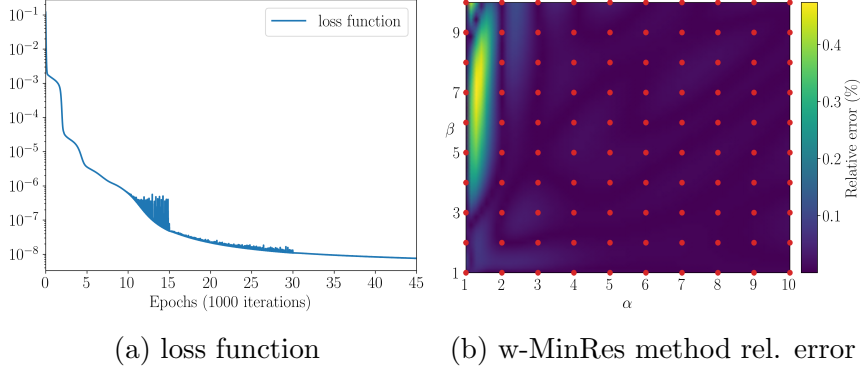


Figure 4: ML-MinRes performance for two-parameters diffusion reaction example. Red dots show the training points.

5.3 1D advection with parametric right-hand side

Let us consider the parametric 1D advection problem:

$$\begin{cases} u_x(x) = f_\lambda(x), & \text{in } (0, 1), \\ u(0) = 0, \end{cases} \quad (20)$$

where $f_\lambda(x) := (x - \lambda)(x > \lambda)$, with $\lambda \in \Lambda := [0, 1]$. We set the quantity of interest as $q(u) = u(0.9)$.

Notice that the exact solution to this problem is

$$u(x) = \begin{cases} (x - \lambda)^2, & \text{if } x > \lambda, \\ 0, & \text{if } x < \lambda. \end{cases}$$

We define the variational formulation,

$$\begin{cases} \text{Find } u \in H_{(0)}^1(0, 1) \text{ such that} \\ \underbrace{\int_0^1 u_x v}_{\langle Bu, v \rangle_{\mathbb{V}^*, \mathbb{V}}} = \underbrace{\int_0^1 f_\lambda v}_{\langle \ell_\lambda, v \rangle_{\mathbb{V}^*, \mathbb{V}}}, & \forall v \in L^2(0, 1), \end{cases} \quad (21)$$

Notice that here $\mathbb{U} = H_{(0)}^1(0, 1)$ and $\mathbb{V} = L^2(0, 1)$. In addition, we use the same inner product defined in (15)-(16), together with the same (discrete) trial space of the previous example in Section 5.1. However, the discrete test space is a piecewise constant space over four uniform elements (same as the weight)⁵.

For this example, we employ the adaptive training set strategy from Subsection 4.1, with 30000 epoch per stage and $\gamma = 5$. We also define the initial training set $\{(\lambda_i, q_{\lambda_i})\}_{i=1}^{N_s}$ composed of $N_s = 11$ elements such that $\lambda_{i+1} - \lambda_i = 0.1$ for all $i \in \{1, 2, \dots, N_s - 1\}$. Notice that some quantities of interest may be zero, so in this case we modify the loss function, by adding a small regularization term

$$\mathcal{L}_{\text{reg}}(\theta; \{\lambda_i, q_{\lambda_i}\}_{i=1}^{N_s}) := \frac{1}{N_s} \sum_{i=1}^{N_s} \frac{1}{2} \left| \frac{q_{\lambda_i} - q(u_{n, \lambda_i}(\theta))}{q_{\lambda_i} + \epsilon_0} \right|^2,$$

where $\epsilon_0 = 10^{-6}$.

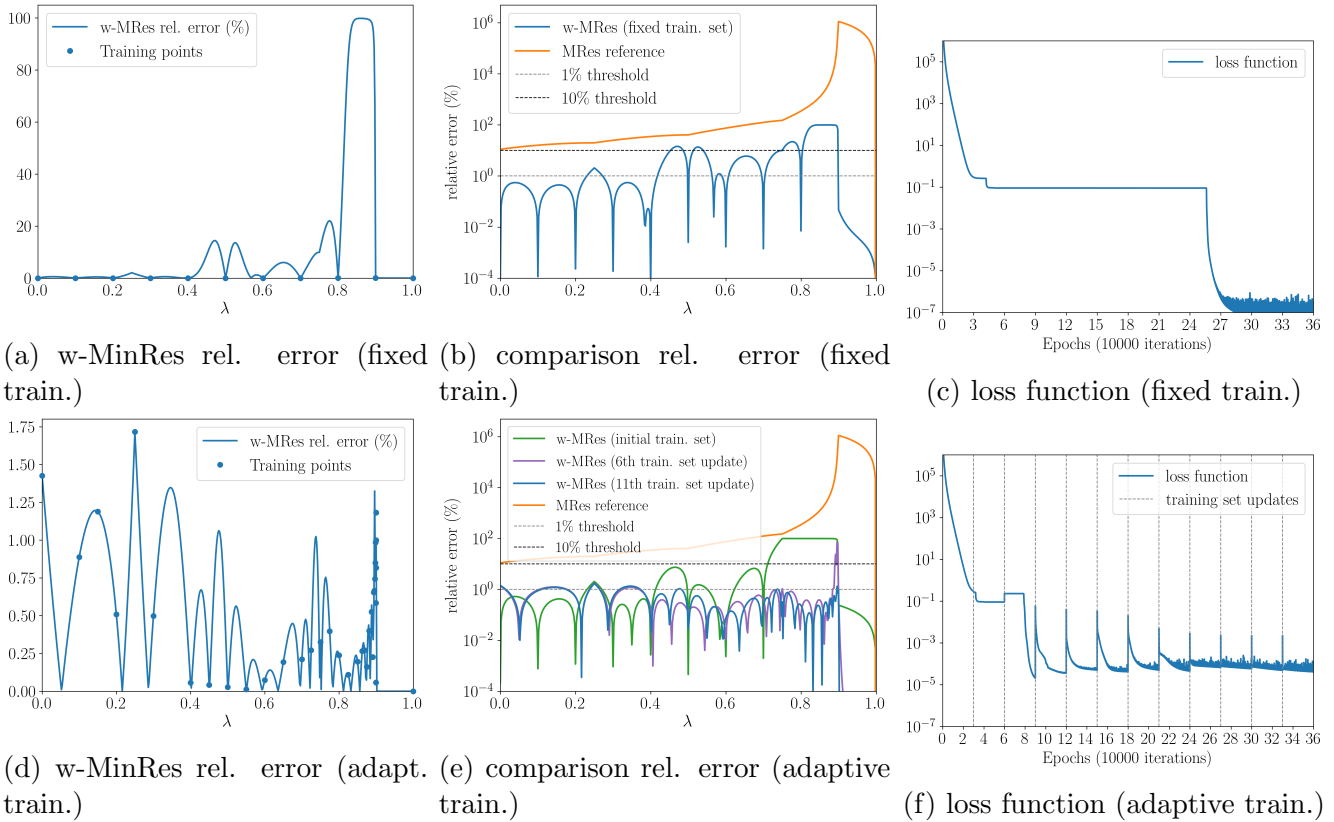


Figure 5: ML-MinRes performance for a 1D advection example with parametric right-hand side. First row shows the results for a fixed training set. The second row displays the results for an adaptive strategy.

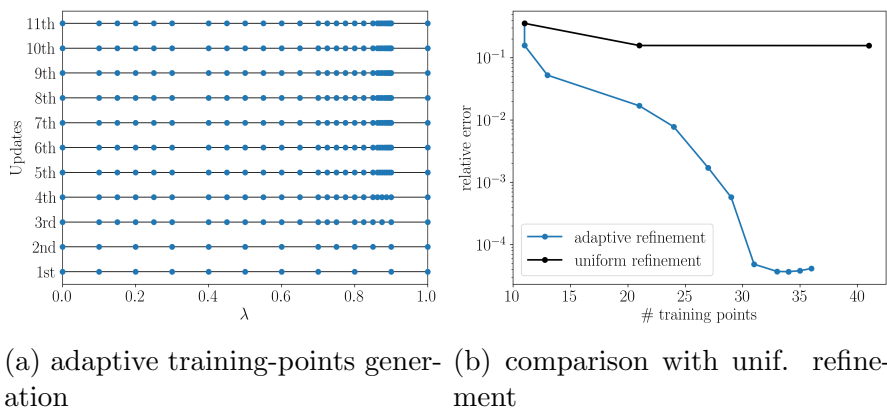


Figure 6: ML-MinRes Adaptive selection of training set and a comparison with uniform refinement for a 1D advection example with parametric right-hand side.

Figure 5 shows the results for the ML-MinRes with a fixed trained set (first row) and with the adaptive training set strategy (second and third rows) presented in Subsection 4.1. Subfigures in the first column show the the relative error in linear scale for the training with a fixed training set (Subfigure 5a) and the adaptive training set (Subfigure 5d). Subfigures 5b and 5e compare the relative error in logarithmic scale between MinRes and ML-MinRes with fixed and adaptive training set. The last column displays the loss function for both cases. Notice that in this example, the fixed training set with eleven elements poorly captures the quantity of interest behavior. This is because the training set does not represent the map between λ and the quantity of interest. Then, the relative error increases drastically between 0.8 and 0.9 (see Subfigure 5a), even when the loss function is small. Then, the adaptive training set emerges as a good alternative to overcome the problem in this type of scenarios.

Finally, the Figure 6 shows the adaptive training-points generation, and a comparison with uniform refinement. In Subfigure 6b we can see the behaviour of the relative error for a test set (different from the adaptive training set) when we add points to the training set with adaptive (blue line) and uniform (black line) refinements after 30000 epoch per refinement.

5.4 2D discontinuous-media diffusion equation with two parameters

Now, we consider a 2D diffusion equation, where the thermal conductivity is given by a two-dimensional parameter $\lambda = (\lambda_1, \lambda_2)$. Thus, we have the following problem:

$$\begin{cases} -\nabla \cdot (a(x, y)\nabla u) = 1, & \text{in } \Omega := (0, 1)^2, \\ u = 0, & \text{on } \partial\Omega, \end{cases} \quad (22)$$

where

$$a(x, y) = \begin{cases} \lambda_1, & \text{if } (x, y) \in \Omega_1 \cup \Omega_3, \\ \lambda_2, & \text{if } (x, y) \in \Omega_2 \cup \Omega_4, \end{cases}$$

with $\Omega_1 = (0, 0.5)^2$, $\Omega_2 = (0.5, 1) \times (0, 0.5)$, $\Omega_3 = (0, 0.5) \times (0.5, 1)$, and $\Omega_4 = (0.5, 1)^2$. See Subfigure 7a.

Here, the quantity of interest is given by

$$q(u) = \frac{1}{\Omega_0} \int_{\Omega_0} u,$$

where, $\Omega_0 = (0.9375 - \frac{1}{2^6}, 0.9375 + \frac{1}{2^6}) \times (0.625 - \frac{1}{2^6}, 0.625 + \frac{1}{2^6})$.

Given the continuous trial and test spaces $\mathbb{U} = \mathbb{V} = H_0^1(\Omega)$, we can obtain the following variational formulation:

$$\begin{cases} \text{Find } u \in \mathbb{U} \text{ such that:} \\ \lambda_1 \underbrace{\int_{\Omega_1 \cup \Omega_3} \nabla u \cdot \nabla v}_{\langle B_1 u, v \rangle_{\mathbb{V}^*, \mathbb{V}}} + \lambda_2 \underbrace{\int_{\Omega_2 \cup \Omega_4} \nabla u \cdot \nabla v}_{\langle B_2 u, v \rangle_{\mathbb{V}^*, \mathbb{V}}} = \underbrace{\int_{\Omega} v}_{\langle \ell, v \rangle_{\mathbb{V}^*, \mathbb{V}}}, \quad \forall v \in \mathbb{V}. \end{cases} \quad (23)$$

Thus, we define $B_\lambda : \mathbb{U} \rightarrow \mathbb{V}^*$ as $B_\lambda := \lambda_1 B_1 + \lambda_2 B_2$. Additionally, we define the following weighted inner product:

$$(r, v)_{\omega_{pw}} := \int_{\Omega} \omega_{pw} \nabla r \cdot \nabla v, \quad \forall r, v \in \mathbb{V},$$

⁵Notice that in this particular example, there is no need to discretize the test space because we can treat the problem using a weighted least squares approach (see [3, Section 3.1])

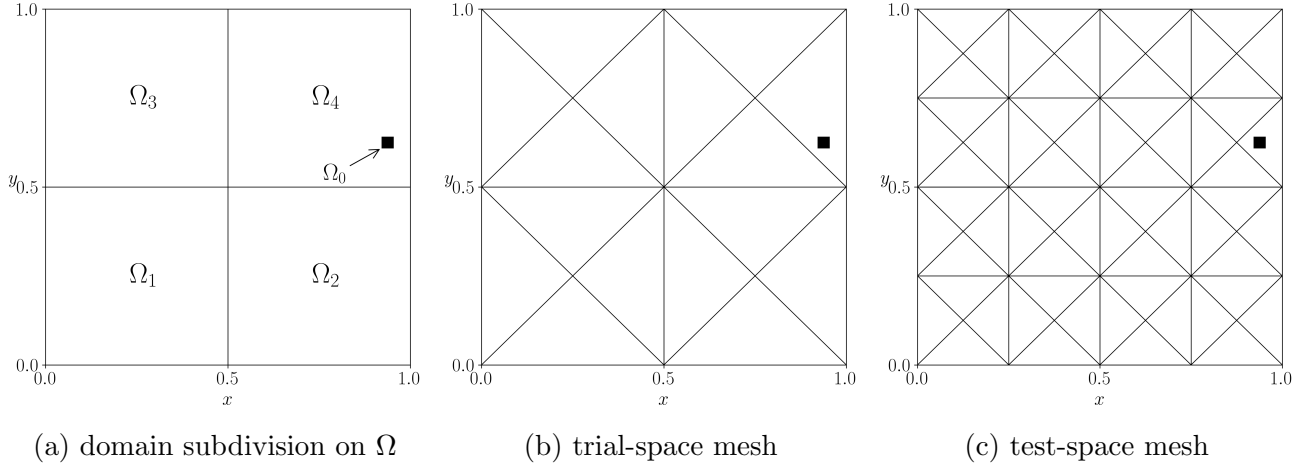


Figure 7: Domain subdivision and meshes for discretization. Back square represents the QoI location.

where ω_{pw} is a constant value on each element of the test-space mesh (64 constants, see Figure 7c).

The discrete trial space \mathbb{U}_n is given by piecewise linear functions with $n = 5$ on a coarse mesh (see Figure 7b), while the discrete test space \mathbb{V}_m is given by piecewise linear functions with $m = 25$ on the mesh depicted in Figure 7c.

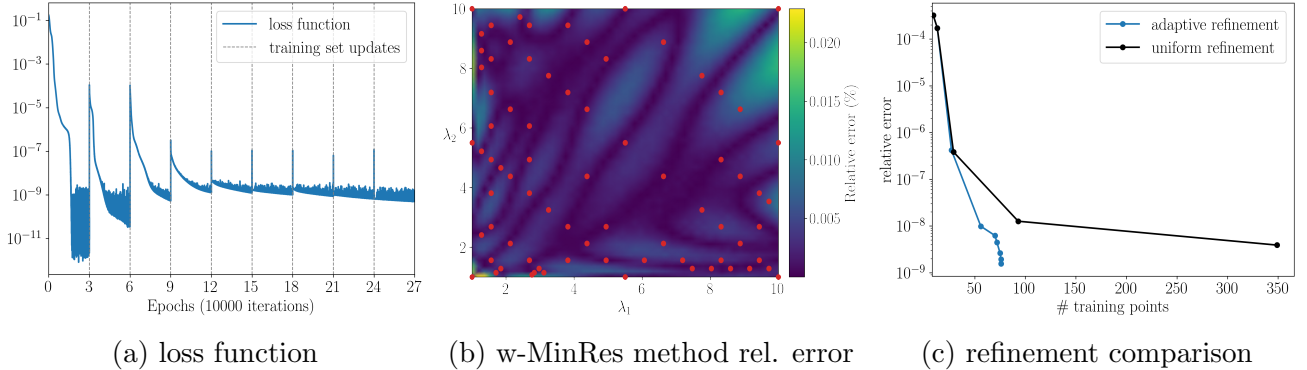


Figure 8: ML-MinRes performance for two-parameters diffusion reaction example. Red dots show the training points.

On this example, we employ the adaptive adaptive training set with eight stages, 30000 epoch per stage and $\gamma = 5$. We also define the initial training set composed of $N_s = 9$ elements, composed by $\{1, 5.5, 10\} \times \{1, 5.5, 10\}$ (Cartesian product).

Figure 8 displays the results for the ML-MinRes after training with an adaptive training-set strategy. Subfigure 8a displays the loss function through the six stages of the adaptive training. Subfigure 8b shows the the relative error (%) in linear scale for full test set after the training with an adaptive training set. Red dot represent the final training set. In Subfigure 8c we can compare the behaviour of the relative error of a test set when we add points to the training set with adaptive (blue line) and uniform (black line) refinements after 30000 epoch per refinement.

6 Conclusions

In the present work, we extend the Machine Learning Minimal-Residual (ML-MinRes) method [2] and [3] to a more general framework of parametric PDEs. The main idea is to compute some high-precision quantity of interest of the solution using finite-element coarse meshes. This finite element scheme will generate a cheap and accurate method for the quantity of interest. As part of the main new features, we highlight the following:

- We avoid the problem of integrating a neural network by replacing the inner-product weight with a piecewise-polynomial weight (with coefficients delivered by a neural network). In this way, we have exact integration with quadrature rules.
- The piecewise polynomial weight for the inner product and the affine decomposition for B_λ and ℓ_λ allow to pre-assemble the matrices. This fact helps to perform more efficient training and faster online evaluation after training.
- We propose an adaptive training set that allows for faster and more accurate neural network training. From the numerical experiments, we can see that adaptive training performs better than uniform refinements. In addition, it helps to reduce overfitting.

Acknowledgements

This publication has received funding from the European Union’s Horizon 2020 research and innovation programme under the Marie Skłodowska-Curie grant agreement No 777778 (MATHROCKS). IB has also received funding from ANID FONDECYT/Postdoctorado No 3200827 and the Engineering and Physical Sciences Research Council (EPSRC), UK under Grant EP/W010011/1. DP has received funding from: the Spanish Ministry of Science and Innovation projects with references TED2021-132783B-I00, PID2019-108111RB-I00 (FEDER/AEI) and PDC2021-121093-I00 (MCIN / AEI / 10.13039/501100011033/Next Generation EU), the “BCAM Severo Ochoa” accreditation of excellence CEX2021-001142-S / MICIN / AEI / 10.13039/501100011033; the Spanish Ministry of Economic and Digital Transformation with Misiones Project IA4TES (MIA.2021.M04.008 / NextGenerationEU PRTR); and the Basque Government through the BERC 2022-2025 program, the Elkartek project SIGZE (KK-2021/00095), and the Consolidated Research Group MATHMODE (IT1456-22) given by the Department of Education. KvdZ was supported by the Engineering and Physical Sciences Research Council (EPSRC), UK under Grant EP/T005157/1 and EP/W010011/1.

References

- [1] K. BHATTACHARYA, B. HOSSEINI, N. B. KOVACHKI, AND A. M. STUART, *Model reduction and neural networks for parametric PDEs*, The SMAI journal of computational mathematics, 7 (2021), pp. 121–157.
- [2] I. BREVIS, I. MUGA, AND K. G. VAN DER ZEE, *A machine-learning minimal-residual (ML-MRes) framework for goal-oriented finite element discretizations*, Comput. Math. Appl., 95 (2021), pp. 186–199. Recent Advances in Least-Squares and Discontinuous Petrov–Galerkin Finite Element Methods.
- [3] I. BREVIS, I. MUGA, AND K. G. VAN DER ZEE, *Neural control of discrete weak formulations: Galerkin, least-squares and minimal-residual methods with quasi-optimal weights*, Comput. Methods Appl. Mech. Engrg., 402 (2022), p. 115716.
- [4] A. COHEN, W. DAHMEN, AND R. DEVORE, *State estimation – the role of reduced models*, in Recent Advances in Industrial and Applied Mathematics, ICIAM 2019, T. C. R. et al., ed., SEMA SIMAI Springer Series 1, Springer, 2022, pp. 57–77.
- [5] L. DEMKOWICZ AND J. GOPALAKRISHNAN, *A class of discontinuous Petrov–Galerkin methods. II. Optimal test functions*, Numer. Methods Partial Differential Equations, 27 (2011), pp. 70–105.
- [6] L. DEMKOWICZ AND J. GOPALAKRISHNAN, *Discontinuous Petrov-Galerkin (dpg) method*, in Encyclopedia of Computational Mechanics, E. Stein, R. de Borst, and T. J. R. Hughes, eds., vol. Part 2 Fundamentals, Wiley, 2nd ed., 2017, pp. 59–137.
- [7] J. FRANKE AND M. H. NEUMANN, *Bootstrapping neural networks*, Neural computation, 12 (2000), pp. 1929–1949.
- [8] S. FRESCA, L. DEDÉ, AND A. MANZONI, *A comprehensive deep learning-based approach to reduced order modeling of nonlinear time-dependent parametrized PDEs*, J. Sci. Comput., 87 (2021).
- [9] M. GEIST, P. PETERSEN, M. RASLAN, R. SCHNEIDER, AND G. KUTYNIOK, *Numerical solution of the parametric diffusion equation by deep neural networks*, J. Sci. Comput., 88 (2021).
- [10] I. GOODFELLOW, Y. BENGIO, AND A. COURVILLE, *Deep Learning*, MIT Press, 2016. <http://www.deeplearningbook.org>.
- [11] I. GÜHRING, M. RASLAN, AND G. KUTYNIOK, *Expressivity of deep neural networks*, arXiv, (2020).
- [12] J. HESTHAVEN AND S. UBBIALI, *Non-intrusive reduced order modeling of nonlinear problems using neural networks*, J. Comput. Phys., 363 (2018), pp. 55–78.
- [13] B. KHARA, A. BALU, A. JOSHI, S. SARKAR, C. HEGDE, A. KRISHNAMURTHY, AND B. GANAPATHYSUBRAMANIAN, *NeuFENet: Neural finite element solutions with theoretical bounds for parametric pdes*. arXiv:2110.01601, 2021.

- [14] Y. KHOO, J. LU, AND L. YING, *Solving parametric pde problems with artificial neural networks*, European Journal of Applied Mathematics, 32 (2021), p. 421–435.
- [15] D. P. KINGMA AND J. BA, *Adam: A method for stochastic optimization*, in 3rd International Conference on Learning Representations, ICLR 2015, San Diego, CA, USA, May 7-9, 2015, Conference Track Proceedings, Y. Bengio and Y. LeCun, eds., 2015.
- [16] G. KUTYNIOK, P. PETERSEN, M. RASLAN, AND R. SCHNEIDER, *A theoretical analysis of deep neural networks and parametric PDEs*, Constr. Approx., 55 (2022), pp. 73–125.
- [17] L. LU, P. JIN, G. PANG, Z. ZHANG, AND G. KARNIADAKIS, *Learning nonlinear operators via deepnet based on the universal approximation theorem of operators*, Nat. Mach. Intell., 3 (2021), p. 218–229.
- [18] S. MISHRA, *A machine learning framework for data driven acceleration of computations of differential equations*, Mathematics in Engineering, 1 (2018), pp. 118–146.
- [19] I. MUGA AND K. G. VAN DER ZEE, *Discretization of linear problems in Banach spaces: Residual minimization, nonlinear Petrov–Galerkin, and monotone mixed methods.*, SIAM J. Numer. Anal., 58 (2020), pp. 3406–3426.
- [20] K. P. MURPHY, *Machine learning: A probabilistic perspective*, MIT Press, 2012.
- [21] M. A. NABIAN, R. J. GLADSTONE, AND H. MEIDANI, *Efficient training of physics-informed neural networks via importance sampling*, Computer-Aided Civil and Infrastructure Engineering, 36 (2021), pp. 962–977.
- [22] E. QIAN, B. KRAMER, B. PEHERSTORFER, AND K. WILLCOX, *Lift & learn: Physics-informed machine learning for large-scale nonlinear dynamical systems*, Physica D: Nonlinear Phenomena, 406 (2020), p. 132401.
- [23] M. RAGHU, B. POOLE, J. KLEINBERG, S. GANGULI, AND J. SOHL-DICKSTEIN, *On the expressive power of deep neural networks*, in Proceedings of the 34th International Conference on Machine Learning, D. Precup and Y. W. Teh, eds., vol. 70 of Proceedings of Machine Learning Research, Proceedings of Machine Learning Research, 2017, pp. 2847–2854.
- [24] D. RAY AND J. S. HESTHAVEN, *An artificial neural network as a troubled-cell indicator*, J. Comput. Phys., 367 (2018), pp. 166–191.
- [25] J. A. RIVERA, J. M. TAYLOR, A. J. OMELLA, AND D. PARDO, *On quadrature rules for solving partial differential equations using neural networks*, Comput. Methods Appl. Mech. Engrg., 393 (2022), p. 114710.
- [26] T. TASSI, A. ZINGARO, AND L. DEDÉ, *A machine learning approach to enhance the SUPG stabilization method for advection-dominated differential problems*, Mathematics in Engineering, 5 (2023), pp. 1–26.
- [27] C. URIARTE, D. PARDO, AND ÁNGEL JAVIER OMELLA, *A finite element based deep learning solver for parametric PDEs*, Comput. Methods Appl. Mech. Engrg., 391 (2022), p. 114562.
- [28] C. WU, M. ZHU, Q. TAN, Y. KARTHA, AND L. LU, *A comprehensive study of non-adaptive and residual-based adaptive sampling for physics-informed neural networks*, Computer Methods in Applied Mechanics and Engineering, 403 (2023), p. 115671.